A New Perspective on Isomerization Dynamics Illustrated by HCN → HNC

Joel M. Bowman* and Bela Gazdy

Cherry L. Emerson Center for Scientific Computation and Department of Chemistry, Emory University, Atlanta, Georgia 30322

Received: February 3, 1997; In Final Form: April 9, 1997⊗

We discuss the role of delocalized states in isomerization dynamics and illustrate the ideas by considering isomerization in HCN. We analyze results from an earlier study, where HCN was treated as a semirigid bender, and isomerization was induced by collision with an Ar atom. That analysis is applied here to three-dimensional HCN, using exact three-dimensional wave functions, obtained using a slight modification of a previous global potential based on high-quality *ab initio* calculations.

I. Introduction

One of the major goals of modern chemical physics is the detailed understanding of elementary chemical reactions in the gas phase. It is generally acknowledged that to achieve this goal success in both experiment and theory is required. Professor Lee and co-workers have been and continue to be world leaders in experimental investigations of such processes.

For a variety of reasons, much experimental and theoretical work has concentrated on bimolecular reactions. The study of unimolecular processes has only recently received a comparable effort; however, the broad class of isomerization reactions has yet to achieve this status. (There are of course well-known technical difficulties in doing this.)

Perhaps the best known system exhibiting isomerization is HCN/HNC. Rigorous quantum treatments of the vibrational states of these isomers have only been achieved in the past 10 years, due to new methods to treat highly excited, floppy systems.[1−8] Most of these calculations (all prior to 1993) used the global potential energy surface for HCN/HNC given by Murrell, Carter, and Halonen.[9] This potential, although optimized to agree with experiment for low-lying HCN vibrational states, has an unrealistically low isomerization barrier. Thus, vibrational calculations using this surface are not realistic for high bend-excited states and certainly are incorrect for delocalized states.

Recently, an accurate fit to high-level *ab initio* calculations was reported for HCN and HNC.[7] This surface does describe the isomerization and does dissociate to H + CN. Vibrational calculations using this surface has also been done for many HCN, HNC, and delocalized states.[7] Agreement with experiment is very good; for 91 experimentally observed states the mean absolute difference between theory and experiment is 21 cm^{-1}. Very recently, this surface (actually a slight modification of it) was adjusted[10] to yield near perfect agreement with experiment.

Isomerization in HCN has also been the focus of many classical and semiclassical studies and several quantum studies. A review of these studies prior to 1993 is given in ref 11, which reported the first use of three-dimensional wave functions to propagate wave packets subjected to an impulse. More recent studies of HCN isomerization include studies based on classical phase space theories[12,13] and light-induced isomerization[14] and a quantum study of collision-induced isomerization of a semirigid bender model of HCN.[15]

In this paper, we review the main point of that quantum study[15] and present a new analysis of it that motivates a detailed examination of delocalized states in the three-dimensional case. On the basis of that analysis, we propose a new perspective on isomerization dynamics, specifically the cumulative isomerization reaction probability.

In the next section of this paper we briefly mention the method we use to obtain highly excited vibrational states of HCN and HNC. Vibrational energies, using a slightly modified version of the previously reported *ab initio* potential,[7] are presented. Energies from calculations of Mandelshtam and Taylor[16] and Wu and Zhang[10] are also presented for this potential surface. Following that, the main body of the paper describes isomerization in terms of delocalized states. Some of these states are presented, and the cumulative isomerization probability is discussed in terms of them.

II. Vibrational Energies

There are a number of methods that can describe both the localized and delocalized states that occur in isomerization. Below we present numerous energies for the HCN/HNC system, using a slight modification of the global *ab initio* potential surface described in ref 7. The slightly modified potential[10] has a very small effect on the localized HCN energies; however, changes of several wavenumbers for HNC states do occur. A new set of vibrational energies from the newer surface were obtained from three groups, using three different methods, and the results are presented below.

The method we used is the same as the one we applied several years ago to HCN/HNC.[7] It is a combination of a truncation/recoupling approach[4] with a movable basis method.[17] Another calculation was done by Mandelshtam and Taylor,[16] who used a novel filter diagonalization method. These calculations are denoted DVR/FD. The third set of calculations was done by Wu and Zhang[10] and was based on an adiabatic sequential-diagonalization procedure.[1,2] These calculations are denoted DVR/TR.

As seen in Table 1, where the calculated energies are given for zero total angular momentum (J), i.e., even bend states only, there is generally very good agreement among the three methods. Table 2 contains energies for the even parity component of $J = 1$, corresponding to the odd bends from two sets of calculations. Again agreement is good. Quantum number assignments have not been given in these tables; however, most of the states that were assigned in ref 7 are quite close in energy to the corresponding states in these tables, and the interested reader may refer to ref 7 for assignments.

⊗ Abstract published in *Advance ACS Abstracts,* July 15, 1997.

S1089-5639(97)00410-6 CCC: $14.00

TABLE 1: Vibrational Energies (in cm^{-1}) for HCN/HNC for $J = 0$

MBM	DVR/TR	DVR/FD	MBM	DVR/TR	DVR/FD	MBM	DVR/TR	DVR/FD	MBM	DVR/TR	DVR/FD
1418.43	1418.40	1418.47	8641.49	8641.31	8641.57	12333.7	12333.4	12333.4	13732.1	13732.1	13731.7
2090.27	2090.41	2090.41	8709.94	8709.62	8709.94	12470.0	12470.3	12470.3	13798.1	13798.0	13798.1
2811.99	2811.97	2812.06	8805.38	8804.99	8805.22	12517.5	12517.1	12517.4	13802.1	13802.3	13802.1
3334.15	3334.16	3334.31	8818.17	8817.96	8818.12	12525.0	12524.6	12524.9	13839.9	13839.7	13839.6
3506.98	3507.00	3507.06	8922.38	8922.51	8922.62	12598.4	12598.7	12598.6	13916.6	13917.7	13916.8
4161.50	4161.50	4161.49	8934.40	8934.32	8934.56	12630.5	12628.3	12628.6	13922.9	13922.5	13922.8
4177.50	4177.44	4177.59	8989.87	8989.71	8989.78	13937.7	13935.6	13935.9	14982.1	14982.9	14982.4
4702.89	4702.93	4703.14	9053.27	9052.89	9052.93	13963.4	13964.4	13963.4	15037.6	15037.8	15037.6
4899.33	4899.27	4899.35	9188.30	9188.00	9188.37	13968.1	13968.0	13968.2	15053.2	15053.7	15053.2
5023.01	5023.07	5023.15	9440.75	9440.54	9440.81	14067.2	14066.9	14067.0	15084.3	15086.7	15084.5
5399.42	5399.20	5399.36	9470.02	9469.71	9470.07	14152.9	14151.3	14151.3	15111.6	15111.6	15111.8
5531.87	5531.71	5531.91	9472.28	9471.61	9471.77	14171.5	14171.0	14171.3	15154.7	15155.2	15154.6
5570.24	5570.01	5570.06	9547.20	9547.02	9547.19	14194.0	14186.7	14186.6	15205.1	15205.7	15205.2
5950.64	5950.55	5950.67	9623.05	9622.75	9622.78	14213.8	14215.0	14213.9	15242.6	15240.7	15240.5
6053.77	6053.45	6053.69	9644.53	9644.19	9644.37	14219.0	14218.9	14219.2	15276.6	15276.9	15276.6
6211.15	6211.19	6211.17	9668.22	9667.88	9668.28	14229.2	14229.7	14229.3	15292.4	15293.4	15292.2
6255.84	6255.82	6255.96	9750.28	9750.23	9750.40	14242.4	14242.0	14242.0	15324.0	15324.3	15323.8
6553.26	6552.98	6553.27	9857.89	9858.04	9858.11	14257.1	14257.4	14257.1	15337.4	15338.4	15337.2
6765.15	6764.97	6765.19	9917.49	9917.08	9917.43	14269.7	14269.4	14269.5	15443.9	15429.6	15429.6
6873.10	6872.81	6873.08	9946.10	9945.71	9945.74	14309.6	14308.7	14308.7	15445.5	15443.2	15442.8
6923.36	6923.33	6923.48	10009.7	10009.3	10009.7	14437.4	14437.7	14437.2	15454.5	15455.8	15454.5
6958.11	6957.92	6958.00	10151.6	10151.1	10151.4	14513.5	14513.9	14513.3	15464.4	15466.1	15464.5
7050.46	7050.66	7050.72	10237.4	10237.3	10237.6	14530.0	14530.7	14530.6	15493.5	15493.4	15492.5
7389.88	7389.64	7389.93	10244.4	10243.4	10243.4	14535.1	14535.5	14535.0	15499.6	15499.7	15499.2
7445.19	7444.96	7445.12	10333.4	10333.2	10333.3	14549.3	14549.4	14549.3	15527.3	15527.3	15526.7
7600.03	7600.03	7600.22	10475.1	10475.0	10475.1	14619.6	14615.9	14616.2	15530.8	15527.5	15527.1
7608.69	7608.56	7608.61	10488.4	10488.2	10488.6	14622.8	14619.8	14619.2	15534.7	15531.3	15530.9
7878.49	7878.17	7878.52	10621.6	10620.9	10621.3	14646.1	14644.7	14644.8	15577.2	15577.2	15577.2
7882.83	7882.79	7882.94	10659.1	10659.0	10659.2	14679.7	14678.6	14679.1	15595.8	15599.1	15595.8
7961.07	7961.27	7961.34	10667.7	10667.6	10667.8	14723.8	14724.3	14723.8	15603.4	15603.0	15603.3
8114.76	8114.55	8114.79	10723.9	10723.6	10723.9	14726.5	14727.8	14726.7	15629.4	15629.2	15628.8
8185.10	8184.83	8185.16	10754.7	10754.5	10754.7	14754.9	14757.1	14754.9	15632.5	15632.8	15632.1
8238.71	8238.57	8238.54	10776.7	10776.9	10776.9	14758.7	14758.8	14758.4	15680.1	15675.2	15675.4
8307.84	8307.54	8307.66	10823.7	10823.0	10823.2	14769.4	14769.0	14768.9	15717.3	15718.8	15717.8
8595.73	8595.35	8595.64	10894.7	10894.4	10894.4	14776.0	14775.6	14775.7	15747.1	15747.9	15747.1
10950.6	10950.2	10950.7	12685.6	12685.2	12685.7	14798.7	14792.1	14792.2	15750.8	15751.1	15750.5
10971.1	10970.8	10971.0	12710.8	12710.7	12710.7	14894.4	14894.7	14894.5	15802.5	15803.1	15802.2
10996.5	10996.1	10996.2	12760.8	12760.7	12760.9	14907.0	14905.4	14905.3	15831.5	15832.1	15831.4
11029.8	11029.2	11029.3	12775.1	12774.7	12775.0	14936.4	14933.9	14933.8	15885.7	15888.7	15885.7
11228.7	11228.2	11228.6	12821.0	12818.7	12818.9	14966.9	14966.2	14966.2	15911.5	15910.9	15910.6
11279.1	11279.0	11279.4	12839.7	12839.6	12839.5	14975.7	14975.6	14975.6	15915.7	15913.8	15911.6
11368.9	11369.0	11368.9	12969.4	12968.8	12969.2	15927.2	15925.2	15924.8	16450.4	16451.9	16450.2
11466.6	11466.4	11466.6	12976.3	12975.5	12975.5	15941.0	15943.1	15941.1	16505.9	16507.4	16505.9
11480.7	11478.6	11478.7	12980.5	12979.8	12979.8	15974.8	15975.1	15974.6	16517.7	16518.0	16516.2
11503.7	11503.8	11503.9	12986.1	12985.7	12985.9	16016.8	16017.9	16017.0	16551.9	16554.1	16551.3
11514.5	11514.0	11514.3	13028.5	13028.3	13028.5	16057.4	16058.3	16057.1	16596.1	16583.2	16583.0
11555.9	11556.0	11556.1	13041.4	13041.5	13041.4	16119.0	16113.3	16112.6	16600.9	16592.5	16592.4
11614.9	11613.8	11613.8	13064.6	13064.7	13064.7	16121.5	16123.0	16121.6	16608.6	16610.1	16608.7
11663.7	11663.5	11663.6	13108.0	13107.7	13108.2	16124.7	16126.3	16124.7	16619.1	16623.9	16619.2
11686.0	11685.4	11685.9	13136.7	13137.3	13136.8	16142.3	16128.0	16127.6	16651.8	16653.9	16651.6
11700.7	11700.9	11700.9	13246.6	13245.9	13246.1	16153.3	16154.9	16153.4	16653.0	16657.2	16652.7
11769.7	11769.6	11769.8	13314.3	13314.2	13314.4	16159.3	16158.4	16158.1	16661.8	16658.5	16658.4
11807.7	11807.5	11807.5	13343.8	13344.7	13344.0	16173.4	16176.3	16173.5	16722.0	16729.5	16722.1
11905.3	11905.0	11905.0	13432.7	13433.2	13432.9	16240.1	16240.1	16239.0	16734.4	16737.9	16734.1
11937.2	11936.5	11936.8	13467.6	13464.7	13464.9	16251.3	16251.9	16250.7	16740.9	16740.8	16738.4
11939.7	11939.1	11939.5	13471.3	13467.2	13467.3	16262.0	16261.6	16260.4	16758.6	16746.3	16744.3
12051.1	12050.8	12051.1	13482.7	13482.6	13482.7	16268.3	16269.3	16268.7	16766.0	16768.3	16765.8
12162.8	12162.5	12162.8	13534.4	13534.2	13534.4	16277.0	16279.4	16277.1	16797.6	16799.1	16797.6
12164.2	12163.4	12163.6	13538.8	13538.3	13538.2	16372.2	16374.8	16372.3	16810.8	16808.3	16807.9
12221.3	12220.9	12221.2	13584.8	13581.9	13581.9	16375.9	16378.3	16375.6	16840.3	16845.7	16840.4
12228.9	12226.0	12225.9	13626.4	13626.3	13626.2	16406.2	16407.8	16405.8	16867.0	16869.3	16867.9
12256.7	12257.0	12256.8	13658.6	13658.3	13658.4	16407.0	16411.5	16407.0	16875.9	16877.5	16875.3
12265.7	12265.2	12265.5	13689.6	13688.1	13688.6	16416.6	16420.2	16416.6			
12301.9	12302.0	12302.0	13726.7	13726.6	13726.7						

III. A New Perspective for the Isomerization Probability

In a previous paper we considered the collision-induced isomerization of HCN, treated approximately as a one-dimensional, semirigid bender.[15] We performed vibrational coupled-channel scattering calculations with Ar as the collision partner and treated the HCN rotation in the infinite-order sudden approximation. The vibrational basis consisted of localized HCN and HNC bending states and delocalized states. The cumulative isomerization probability at the total energy E was defined as

$$N_{\mathrm{iso}}(E) = \sum_{\substack{i \in HCN \\ f \in HCN}} P_{\mathrm{i}\rightarrow\mathrm{f}}(E) \qquad (1)$$

where $P_{\mathrm{i}\rightarrow\mathrm{f}}(E)$ is the state-to-state isomerization probability and the sum is over all initial HCN states and all final HNC states.

TABLE 2: Vibrational Energies (cm^{-1}) of HCN/HNC for $J = K = 1$

MBM	DVR/ TR	MBM	DVR/ TR	MBM	DVR/ TR	MBM	DVR/ TR
718.1	718.0	9097.8	9096.9	11462.9	11461.7	13136.8	13134.9
2125.3	2124.9	9270.2	9269.8	11503.4	11502.3	13169.6	13168.5
2806.2	2806.1	9293.5	9291.1	11592.7	11592.1	13177.7	13175.4
3505.0	3504.4	9371.2	9369.9	11631.2	11628.8	13292.3	13289.9
4034.1	4033.9	9401.8	9400.5	11677.1	11675.7	13298.7	13296.9
4213.3	4212.9	9487.7	9486.9	11821.5	11819.6	13316.6	13316.0
4862.6	4861.8	9496.5	9495.5	11885.9	11884.9	13380.6	13377.6
4872.1	4871.9	9598.4	9596.6	11912.4	11910.7	13404.2	13403.2
5386.6	5386.3	9673.9	9672.7	11918.0	11915.0	13433.5	13431.6
5488.7	5488.0	9848.4	9847.5	12024.1	12022.9	13447.2	13444.2
5588.9	5588.2	10021.2	10019.8	12128.2	12126.7	13492.9	13492.2
6095.0	6094.8	10105.2	10103.9	12151.7	12149.1	13496.9	13494.3
6213.3	6212.0	10111.3	10109.4	12156.7	12154.0	13569.0	13566.9
6273.6	6273.1	10155.8	10155.0	12166.1	12163.7	13613.5	13612.6
6440.2	6439.1	10221.0	10218.3	12266.1	12263.8	13639.1	13636.4
6731.8	6731.1	10315.5	10314.1	12303.6	12301.6	13654.3	13653.1
6915.0	6914.7	10321.5	10319.8	12335.5	12333.2	13656.1	13654.2
6935.4	6934.4	10324.3	10323.8	12341.3	12340.4	13683.2	13680.4
7232.3	7232.0	10325.8	10324.0	12379.7	12378.0	13788.5	13787.4
7414.2	7412.8	10426.7	10425.1	12410.7	12409.4	13844.3	13841.6
7448.7	7448.2	10580.7	10580.0	12540.7	12537.6	13900.0	13898.8
7504.6	7504.3	10656.5	10655.0	12599.7	12598.7	13944.3	13942.6
7541.1	7539.5	10820.2	10819.1	12607.6	12606.8	14000.0	13998.3
7644.9	7643.9	10888.0	10885.8	12695.1	12693.4	14086.9	14084.1
8059.3	8058.3	10932.9	10931.4	12697.3	12694.5	14112.8	14112.2
8135.6	8135.2	10933.3	10931.7	12713.8	12711.4	14125.6	14124.0
8278.4	8276.9	11005.6	11003.8	12826.8	12825.5	14138.1	14131.7
8308.1	8307.3	11101.1	11098.4	12861.5	12860.8	14167.9	14165.9
8360.8	8358.8	11112.7	11111.9	12908.4	12905.6	14180.9	14178.5
8446.8	8445.8	11139.0	11137.9	12912.4	12909.6	14184.4	14181.3
8540.7	8540.2	11248.2	11245.9	12918.3	12917.0	14267.7	14263.8
8788.6	8787.8	11290.5	11289.6	13003.2	13001.1	14307.0	14305.3
8839.7	8837.7	11347.0	11344.3	13036.2	13032.2	14325.8	14323.4
8935.1	8934.5	11363.6	11361.7	13102.5	13101.1	14327.0	14324.4
8983.2	8981.7	11414.7	11413.2				

We did scattering calculations including a large number of delocalized as well as all localized states in the basis, and also for diagnostic purposes, we limited the basis to localized states only. We found that in the tunneling region, i.e., E below the barrier height for isomerization, that the two bases gave nearly identical results for $N_{\rm iso}(E)$. However, for energies above the barrier height (and even slightly below) the calculations with only localized states deviated significantly from the fully converged ones, which contained delocalized states. Thus, we concluded that delocalized states play a major role in the isomerization dynamics for energies above, and even somewhat below, the barrier height. We proposed that the isomerization mechanism was for a delocalized state to be populated in the "first half" of the collision and then depopulated in the "second half" of the collision to form either isomer. (Thus, the process is somewhat like Raman light scattering.)

We now take this qualitative picture one step further and propose the following statistical expression for $N_{\rm iso}(E)$:

$$N_{\rm iso}^{\rm s}(E) = N_{\rm D}(E)\left[\frac{N_{\rm HNC}(E)}{N_{\rm HCN}(E) + N_{\rm HNC}(E)}\right] \tag{2}$$

where $N_{\rm D}(E)$, $N_{\rm HCN}(E)$, and $N_{\rm HNC}(E)$ are the number of delocalized states and the number of HCN and HNC localized states, respectively, at the total energy E.

For the semirigid bender the number of localized states maximizes at the threshold energy of the first delocalized state. At and above that energy all states are delocalized (for the semirigid bender). This expression is clearly a statistical approximation to $N_{\rm iso}(E)$, which in the case of collision-induced isomerization would be almost certainly an upper bound to the true $N_{\rm iso}(E)$. This is because the collisional efficiency to populate a delocalized state from a localized one and then to depopulate the delocalized state to a localized state cannot exceed unity, whereas the above expression assumes unit efficiency for this process.

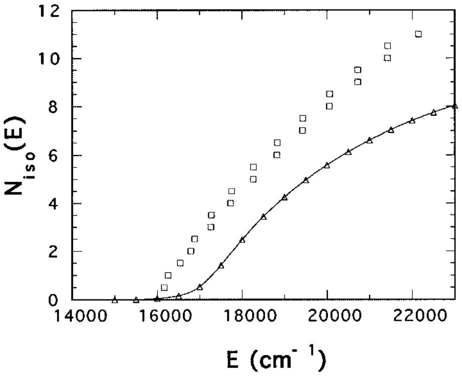

Figure 1. Cumulative isomerization reaction probability for HCN and HNC (treated as a semirigid bender) induced by collision with Ar, $N_{\rm iso}(E)$ (triangles connected by a solid curve), as a function of the total energy E (from ref 11), and the present statistical approximation to $N_{\rm iso}(E)$ (squares) as defined in the text.

A comparison of the previously calculated $N_{\rm iso}(E)$ and the statistical approximation to it is shown in Figure 1. The collisional result is for the zero partial wave of the Ar−HCN system (and also for a fixed orientation of the HCN). In the present case the ratio of HNC localized states to HNC plus HCN localized states is 0.5. Thus, in this case $N_{\rm iso}^{\rm s}(E)$ is half the number of delocalized states.

Note that the threshold for $N_{\rm iso}^{\rm s}(E)$, which is simply the energy of the first delocalized state, 16 161 cm^{-1}, is somewhat below the barrier to isomerization, 16 800 cm^{-1}. Thus, to some extent tunneling is present in the model. (Direct tunneling from a localized HCN state to a localized HNC state is not described by the statistical model; however, it would not be difficult to approximately include that.) As expected, $N_{\rm iso}^{\rm s}(E)$ is larger than the "exact" $N_{\rm iso}(E)$ (about 60% larger in this example); however, the energy dependence of $N_{\rm iso}(E)$ is reasonably well reproduced by the statistical approximation.

Next, consider the extension of the statistical approach to three-dimensional HCN. This extension is relatively straightforward, although there is one major difference with the semirigid bender model discussed above. In contrast to the sharp demarcation in energy between localized and delocalized states in the semirigid bender model, localized and delocalized states coexist even at energies well above the barrier to isomerization in three degrees of freedom. Thus, in principle the phase-space ratio in eq 2 is energy dependent; however, for the present purpose (which is only semiquantitative) we simply use the constant value of 0.34 for the ratio of HNC states to all localized states. This value is the ratio of HNC states to all localized states with energies below the energy of the first delocalized state.

Delocalized states were identified by calculating the expectation value and standard deviation of the angular variable for all wave functions. Those with corresponding values near 90° and 40°, respectively, were identified as delocalized states, and then contour plots were made and examined to verify that they are indeed delocalized. Examples are shown in Figures 2−5. The wave functions in Figures 2 and 3 have energies below the adiabatic barrier height, which in the harmonic approximation for the modes orthogonal to the reaction path is 15 685 cm^{-1}. As seen, these wave functions are completely delocalized over the HCN and HNC minima and are nodeless in the H−CN stretch. Consider, next, two higher energy delocalized states,

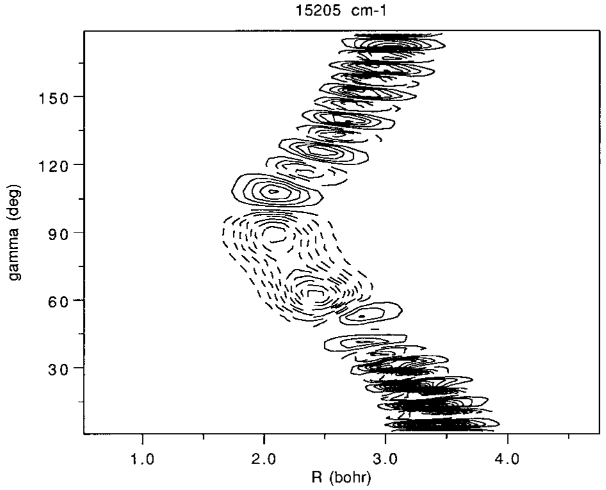

Figure 2. Contour plot of the lowest energy delocalized state as a function of the distance of H to the center of mass of CN, R, and γ, the angle between the vector $\mathbf{R}$ and the CN bond, which is fixed in this plot at a bond length of 2.19 bohr.

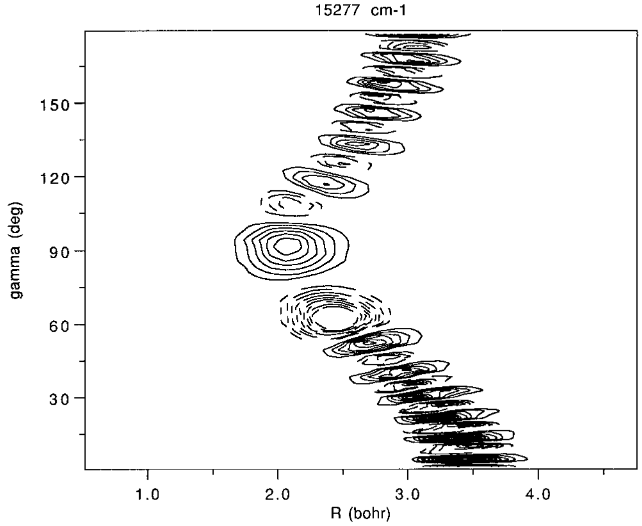

Figure 3. Same as Figure 2 but for the next delocalized state in energy.

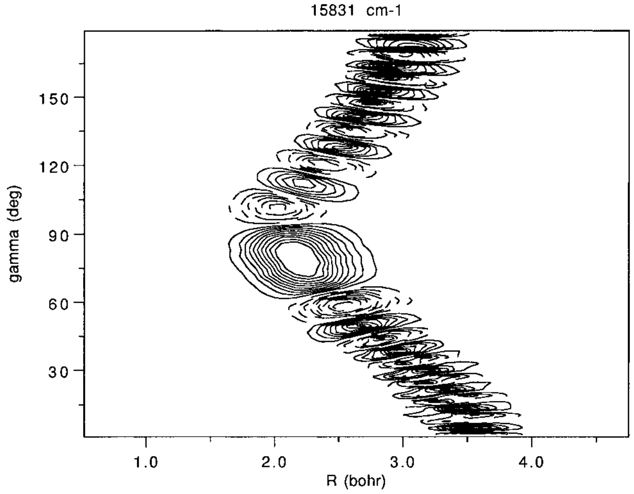

Figure 4. Same as Figure 3, but for the first delocalized state with energy above the adiabatic barrier for isomerization.

shown in Figures 4 and 5. The higher of this pair, shown in Figure 5, has a very interesting nodal structure. There is a node in the H−CN stretch in the HNC well, but not in the HCN well. This delocalized wave function is clearly is not adiabatic in the H−CN stretch.

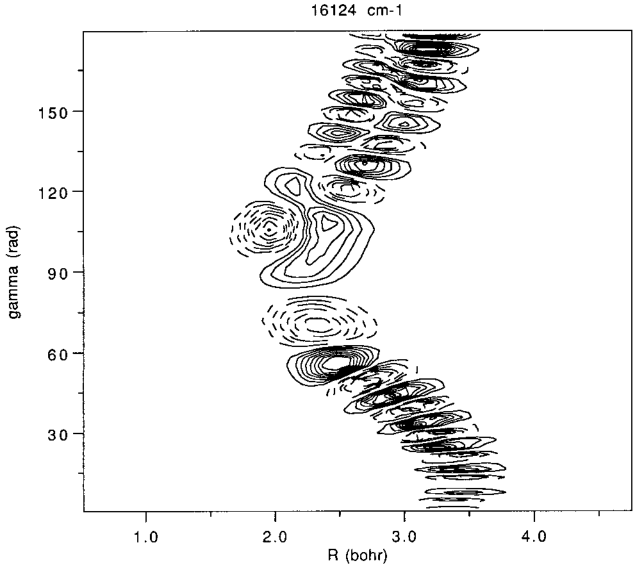

Figure 5. Same as Figure 2, but for a higher energy state.

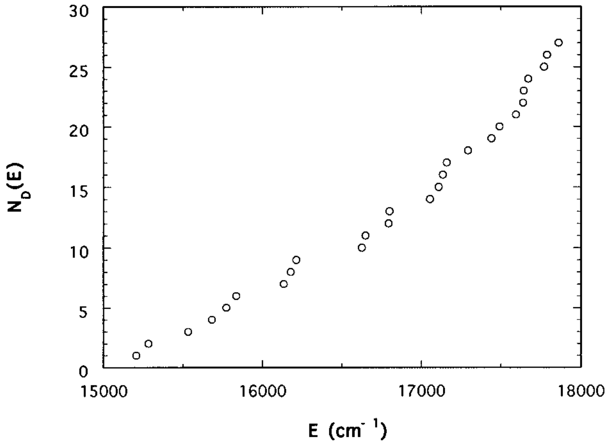

Figure 6. Number of delocalized HCN/HNC states as a function of energy (measured with respect to the HCN zero-point energy).

Finally, we plot in Figure 6 the number of delocalized states, $N_D(E)$, as a function of the energy, measured with respect to the HCN zero-point energy. The statistical approximation to $N_{iso}(E)$ would be simply $0.34N_D(E)$.

The result in Figure 6 is for zero total angular momentum J equal to zero and 1 (but only for the even parity state). In order to obtain $N_D(E)$ exactly for higher values of J, it would be necessary to repeat the vibrational calculation for each J. A simpler approach would be to use J shifting, which has been shown to be quite useful in bimolecular reactive scattering.[18] In this approximation

$$N_D^{J,K}(E) \approx N_D^{J=K=0}(E - E_{JK}^{\ddagger})$$

where $E_{JK}^{\ddagger}$ is the rotational energy of the HCN/HNC transition state.

IV. Summary

We have shown that there is a strong correlation between the cumulative reaction probability for isomerization and the number of quantum delocalized states. This correlation was demonstrated for HCN, where isomerization was induced by collision with Ar. The delocalized states mediate the isomerization by being temporarily populated during the interaction that induced the isomerization. Further, we proposed a simple statistical model to obtain essentially an upper bound to the cumulative isomerization probability. The model assumes that delocalized states relax to a stable isomer with a probability given by relative phase space occupied by that isomer at a given total energy.

This simple proposal was tested for Ar−HCN, where HCN was treated as a semirigid bender. The statistical result exceeded the collisional one as expected, because the efficiency to make a transition from localized states to delocalized states and back to localized states is assumed implicitly to be unity in the statistical theory. It is in this sense that the statistical theory is characterized as essentially an upper bound to the correct result.

Acknowledgment. Partial support from the National Science Foundation (CHE-940815030) is gratefully acknowledged. We are grateful to Vladimir Mandelshtam, Howard Taylor, Qian Wu, and John Zhang for their sending us their calculated vibrational energies of HCN/HNC.

References and Notes

(1) (a) Bacic, Z.; Light, J. C. *J. Chem. Phys.* **1987**, *86*, 3065. (b) Light, J. C.; Bacic, Z. *J. Chem. Phys.* **1987**, *87*, 4008.

(2) (a) Mladenovic, M.; Bacic, Z. *J. Chem. Phys.* **1990**, *93*, 3039. (b) Bacic, Z. *J. Chem. Phys.* **1991**, *95*, 3456.

(3) (a) Brunet, J.-P.; Friesner, R. A.; Wyatt, R. E.; Leforestier, C. *Chem. Phys. Lett.* **1988**, *153*, 425. (b) Bentley, J. A.; Brunet, J.-P.; Wyatt, R. E.; Friesner, R. A.; Leforestier, C. *Chem. Phys. Lett.* **1989**, *161*, 393. (c) Bentley, J. A.; Huang, C.-M.; Wyatt, R. E. *J. Chem. Phys.* **1993**, *98*, 1993.

(4) (a) Gazdy, B.; Bowman, J. M. *Chem. Phys. Lett.* **1990**, *175*, 434. (b) Bowman, J. M.; Gazdy, B. *Theor. Chim. Acta* **1991**, *79*, 215. (c) Bowman, J. M.; Gazdy, B. *J. Chem. Phys.* **1991**, *95*, 6309.

(5) (a) Leforestier, C. *J. Chem. Phys.* **1991**, *94*, 6388. (b) Menou, M.; Leforestier, C. *Chem. Phys. Lett.* **1993**, *210*, 294.

(6) Friesner, R. A.; Bentley, J. A.; Menou, M.; Leforestier, C. *J. Chem. Phys.* **1993**, *99*, 308.

(7) (a) Bowman, J. M.; Gazdy, B.; Bentley, J. A.; Lee, T. J.; Dateo, C. E. *J. Chem. Phys.* **1993**, *99*, 308. (b) Bentley, J. A.; Bowman, J. M.; Gazdy, B.; Lee, T. J.; Dateo, C. E. *Chem. Phys. Lett.* **1992**, *198*, 563.

(8) Bramley M. J.; Carrington, Jr., T. *J. Chem. Phys.* **1994**, *101*, 8494.

(9) Murrell, J. N.; Carter, S.; Halonen, L. O. *J. Mol. Spectrosc.* **1982**, *93*, 307.

(10) Wu, Q.; Zhang, J. Z. H.; Bowman, J. M. *J. Chem. Phys.*, in press.

(11) Lan, B. L.; Bowman, J. M. *J. Phys. Chem.* **1993**, *97*, 12353.

(12) DeLeon, N.; Ling, S. *J. Chem. Phys.* **1994**, *100*, 4790.

(13) Tang, H.; Jang S.; Zhao, M.; Rice, S. A. *J. Chem. Phys.* **1994**, *101*, 8737.

(14) Dion, C. M.; Chelkowski, S.; Bandrauk, A. D.; Umeda, H.; Fujimura, Y. *J. Chem. Phys.* **1996**, *105*, 9083.

(15) Lan, B. L.; Bowman, J. M. *J. Chem. Phys.* **1994**, *101*, 8564.

(16) Mandelshtam, V. A.; Taylor, H. S. *J. Chem. Phys.*, submitted.

(17) Bowman, J. M.; Gazdy, B. *J. Chem. Phys.* **1990**, *93*, 1774.

(18) (a) Bowman, J. M. *J. Phys. Chem.* **1991**, *95*, 4960. (b) Sun, Q.; Bowman, J. M.; Schatz, G. C.; Connor, J. N. L. *J. Chem. Phys.* **1990**, *92*, 1677.